An Advanced Power Converter System Based on High Temperature, High Power Density SiC Devices[1]

Timothy (Zhigang) Lin (Aegis Technology Inc., Santa Ana, California, USA) aegiste1400@earthlink.net; Bob Liu (Aegis); Hui Zhang, Tolbert Leon (The University of Tennessee at Knoxville)

1. Introduction

SiC power devices have the potentials for reliable operations at higher junction temperatures, higher voltages, higher frequencies and thus higher power densities than these that can be achieved with Si devices [1-8]. These advantages are enabling the SiC technology-based power conversion systems (PCM) to be made smaller, lightweight, more efficient and robust [9-15]. Recent studies predicted that the volume of a power converter system could be reduced five times through the utilization of SiC power devices [14]. Despite these promising potentials and encouraging results, more studies addressing the design and fabrication of SiC-based PCMs are anticipated before their potentials can be fully realized. Currently there exist two major technical issues that need well addressing in order to fully exploit the potential offered by SiC technologies. They are: (1) Benefits, circuit designs and modeling of the utilization of SiC devices in a system level [6, 7, 9, 12, 13]; and (2) Thermal management that can take advantage of SiC's high-temperature, high-voltage, high power density capabilities [14-16]. Challenges in applying SiC power devices for commercial utilities include the high cost (expensive material, low yield) and limited availability (Schottky diodes, JFET) of SiC devices [9-13], and a need of passive components and gate drivers suitable for SiC devices [12,17].

Being sponsored by U.S. DOE through a STTR/SBIR program, currently Aegis Technology is developing and demonstrating a high-efficiency compact power converter system based on emerging SiC semiconductor technologies, quantifying the system benefits and addressing the related technical issues. The SiC-based converter with a scalable current rating will be inserted for the applications in electric energy storage, motor control, and others. At present the impact of using SiC devices in an all-SiC converter design has been evaluated in terms of power loss. A novel high temperature, high power density package for SiC power devices has also been developed. This paper presents the major results in this development, including: (1) Circuit design and modeling of converter to evaluate the effects of SiC devices on power loss and efficiency; and (2) High temperature, high power density packaging techniques to support the SiC converter.

2. Circuit design

A 3-phase inverter of 1200 V, 20 A is designed, by using the common inverter design as adopted by a modern 3-phase Si inverter driving an induction machine load (Figure 1). One targeted application of inverter is for a battery energy storage system (Figure 2).

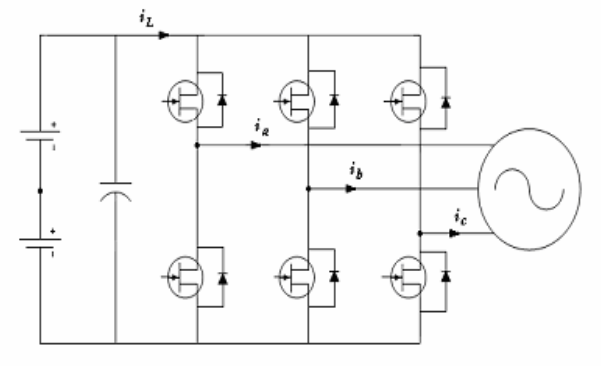

Figure 1. A 3-phase inverter driving an induction machine load

[1] Funded by the Energy Storage Systems Program of the U.S. Department Of Energy (DOE/ESS) through the Small Business Innovation Research (SBIR) program and managed by Sandia National Laboratories (SNL).

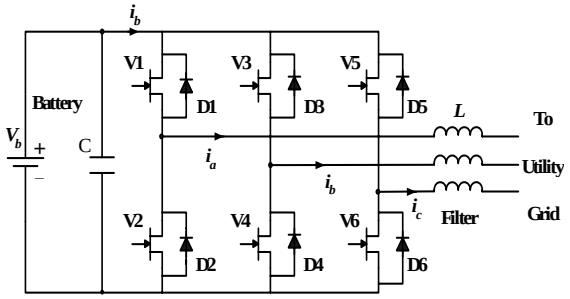

Figure 2. A battery converter design for utility grid

The circuit design of SiC power module is shown in Figure 3. It is a 6-packed design, consisting of six switch (JFET arrays) and six anti-parallel diodes (diode arrays). The feed throughs of 1, 2, 3, 4, and 5 are for the power input and output, and the feed throughs of 9 though 17 are for the circuit control. In the circuit, the upper VJFETs conduct when the load current is positive, while the lower VJFETs conduct when the load current is negative. For each direction of the current, only one of the two anti-parallel elements conducts. Because of the limited current values of available SiC devices, multiple chips needs to be used in parallel.

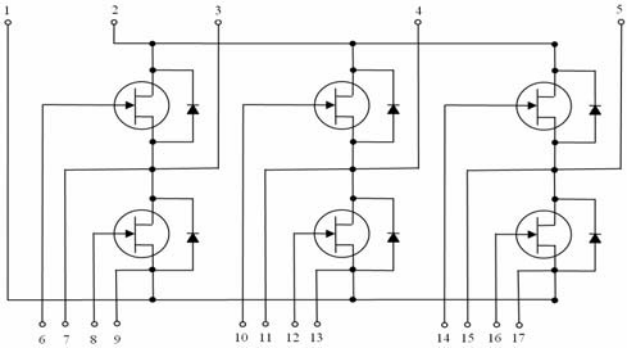

Figure 3. Power module with fed-through layout

3. Thermal management and package

Thermal management of SiC power module, including the package and its heatsink, is a key issue of the SiC-based inverter [14, 16]. Our thermal management technique is based on: (1) a novel AlN high temperature package, (2) a high-efficiency graphite foam heatsink, and (3) a novel package structure to integrate the package and heatsink. The thermal management will be capable of withstanding high temperature operations with high-efficiency heat dissipation, and hence a conventional bulky fluid-cooling can be replaced with a simple air-cooling. A thermal package design for SiC power module is shown in Figure 4. SiC chips are attached on the AlN substrate. The substrate is then bonded to the heatsink made of carbon foam. The heatsink can be used for both an air cooling and a liquid cooling. We focus on an air-cooling heatsink, as it is likely to be sufficient for the heat dissipation in the proposed application, on account of a unique combination of a high-efficiency heatsink with a high-temperature operation of SiC devices.

An AlN ceramic substrate is selected, because of its advantages including high thermal conductivity, low CTE (Coefficient of thermal expansion) matchable with SiC, and high thermal shock resistance and insulation. The properties of AlN as compared to the conventional alumina are shown in Table 1 [16]. The metallization of the AlN substrate is needed for circuit patterns, die attachment and bonding with heatsink. Since the common metallization of direct-bonded copper on AlN ceramic oftentimes is not robust enough to withstand high temperature [14], a proprietary metallization method is utilized, which can withstand a temperature up to 600C.

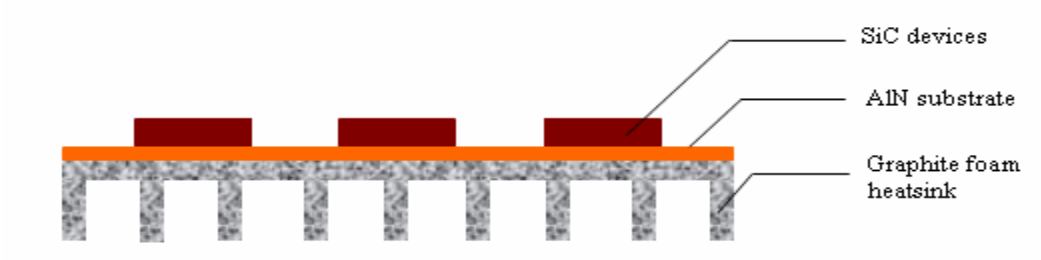

Figure 4. Thermal package design for SiC power module

Table 1 Some properties of carbon foam as compared with solid Al and Cu

	AlN	Alumina
Thermal conductivity (W/m K)	170 - 200	20
Dielectric strength (kV/cm)	140 - 170	100
CTE (x10-6/°C) (25 ~ 400 °C)	4.5	7.3
Density (g/cm3)	3.3	3.9
Flexure strength (MPa)	300 - 500	240 - 260

Carbon foam material with high thermal conductivity is used for the heat sink. The carbon foam has a high population of pores, or so-called open cells. The open cells are interconnected to form a complicated 3-dimension network. When liquid or air coolant is forced through numerous interconnected irregular open cells, an intensive convective cooling can be achieved. Compared to a common microchannel cooling or plate-fin heatsink, a carbon foam heatsink has the advantages of much larger surface area for convective heat transfer. The larger specific surface area offers a much-enhanced convective heat transfer and thus a higher heat flux capability. In addition, the cell walls of carbon foam are made of oriented graphitic-like planes, similar to graphite fibers, and it is estimated that the thermal conductivity of the cell walls is 1500-1800 W/m·K (copper is 400 W/m·K). The following Table 2 shows the advantages of carbon foam material as compared with other materials [14, 18]. The overall heatsink transfer coefficients of carbon foam heatsink can be substantially greater than conventional solid heatsink. A recent investigation on a carbon foam heatsink has demonstrated over 100% enhancement in heat transfer over an aluminum heatsink (To be published in another paper).

Table 2 Some properties of carbon foam as compared with solid Al and Cu

	Porosity [%]	Ligament Density* [g/cc]	Bulk Density [g/cc]	Ligament thermal Conductivity [W/m.k]	Bulk thermal Conductivity [W/m.k]
Solid Aluminum	0	2.8	2.8	180	180
Solid Copper	0	8.9	8.9	400	400
Carbon foam	61	2.3	0.9	1800	150

4. Modeling and simulation

Based on the power loss models (conduction loss and switching loss), the power losses of individual SiC device and the resultant power module are computed. By calculating the junction temperatures of the SiC devices and the energy efficiency of the inverter, the advantages of the SiC inverter compared to its Si counterpart are evaluated quantitatively in terms of junction temperature, power loss and energy efficiency. To investigate the long-time performance of SiC devices, a periodical input is modeled to compute the junction temperature increase of devices. This modeling and simulation, which are in both device level and system level, can also be used to study the feasibility of SiC circuit design.

Since the power losses of the devices and their dependence on temperature determine the system performance, it is essentially necessary to do a detailed study about the device power losses. The power losses of two devices, SiC VJFET and Schottky diode are modeled. A VJFET has two kinds of losses, conduction loss and switching loss. The VJFET's conduction losses consist of the resistive losses of itself and the losses associated with the reverse current of diodes. Because of no reverse recovery current in VJFET, its switching losses only consist of turn-on and turn-off energy losses. Similarly with VJFET, the losses of a Schottky diode are also composed of both conduction and switching losses. Unlike JFETs, the resistive loss is not the only loss in a Schottky diode. The loss due to the junction voltage drop also contributes to the total losses. Generally the reverse recovery loss dominates its switching losses. Therefore in the modeling, the other losses can be neglected and only the reverse recovery loss is considered.

4.1 Power loss and thermal model

Regarding the thermal modeling, a direct method that computes thermal information based on the power loss of an equivalent circuit is used. The total power loss of the power is equal to the sum of the power loss of each VJFET and diode. It can be expressed as

$$P_{tot} = (P_J + P_D) \times 6 \tag{1}$$

P_J is the power loss of VJFETs, which includes a conduction loss (part of it is due to diodes' reverse recovery current) and a switching loss,

$$P_J = P_{cond,J} + P_{cond,D \to J} + P_{sw,J}, \tag{2}$$

P_D is the power loss of Schottky diodes, which also includes a conduction loss and a switching loss,

$$P_D = P_{cond,D} + P_{sw,D} \tag{3}$$

The thermal model of each switch is shown in Figure 5. It can be represented by

$$Z_{jc}(s) = \frac{R_1}{1 + s\tau_1} + \frac{R_2}{1 + s\tau_2} + \cdots + \frac{R_3}{1 + s\tau_3} \tag{4}$$

where $\tau_i = R_i C_i$ and the junction-case thermal resistance $R_{jc} = \sum_{i=1}^{n} R_i$. The thermal model for the entire system can be shown as Figure 6.

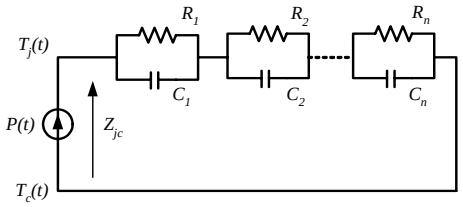

Figure 5. A single switch thermal model

Figure 6 shows the thermal model for the entire converter system. $P_j(t)$ and $P_d(t)$ are the total power losses generated by a VJFET and a Schottky diode, respectively. It is assumed that the VJFET and the Schottky diode are mounted on the same heatsink, and the power losses $P_j(t)$ and $P_d(t)$ flow through separate paths from their own junction to case, where the temperatures are equal for contacting to the same heatsink. Afterwards, they merge with each other ($P_j(t) + P_d(t)$) and flow together through the heatsink to the ambient environment.

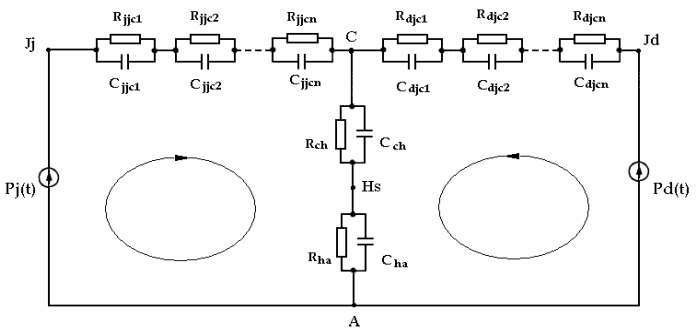

Figure 6. The thermal equivalent circuit of the inverter module

4.2 Simulation

The simulation of the above models is implemented using Matlab Simulink. The simulation on a drive system has been conducted, and currently the simulation for the batter system is ongoing. Their simulation flowcharts are shown in Figure 7. In the following the simulation results based on Fig. 7a are presented.

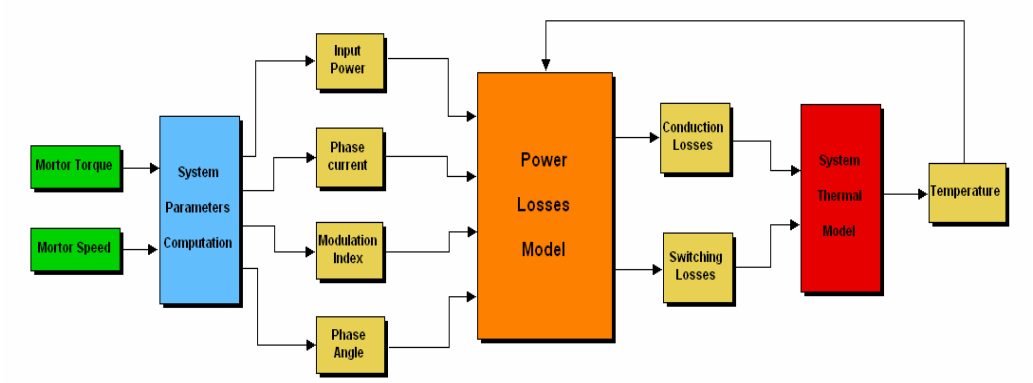

(a) A drive system

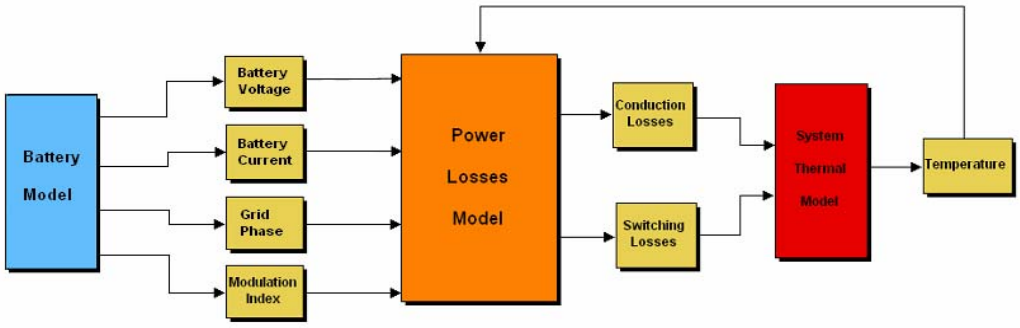

(b) A battery system

Figure 7. Simulink flowchart for the simulation of three-phase SiC inverters

Based on the above modeling, a simulation is done on a drive system, whose parameters are shown in Figure 8. Figure 9 shows the devices temperature for a SiC JFET inverter, which has the same cooling condition and ambient temperature as a Si MOSFET-based inverter. The thermal resistance and thermal time constant of the

heat sink are: R_{ca}= 0.1 K/W and τ_{ca} = 1000 s. Figure 10 shows the power losses of SiC JFETs and SiC Schottky diodes per switch. If this system operates continuously for more than one drive operation, the device temperature will continue increasing with a rate of temperature rise is approximately 0.537°/min (Figure 11). By using a more efficient heatsink, for example, by changing the thermal resistance and capacity from R_{ca}= 0.1 K/W and τ_{ca} = 1000 s to R_{ca}= 0.156 K/W and τ_{ca} = 102 s, the rate of temperature rise will slow down to about 0.051°/min (Figure 12).

Compared to Si MOSFET inverter, the advantage of SiC devices is obvious. The junction temperatures of SiC devices are significantly less than these of Si devices. Table 3 lists the main simulation results such as temperature increase and power loss under two cooling conditions, R_{ca}= 0.156 K/W and τ_{ca} = 102 s (Heatsink1) and R_{ca}= 0.1 K/W and τ_{ca} = 1000 s (Heatsink 2). It shows that the junction temperatures of Si inverter in this operation increase much higher than SiC devices, leading to much higher power losses. The table also shows the difference in the temperature rise per cycle between these two cooling condition. A better-performance heatsink makes a significant contribution for the reduction of an average junction temperature particularly for the switch devices -- changing from Heatsink 1 to Heatsink 2, the average junction temperature average is reduced by a factor of 9 to 10 for JFETs/MOSFETs and 1.3 to 2.6 for diodes. It is also illustrated that the improvement of cooling condition does not affect the peak junction temperatures very significantly, but it significantly reduces the average junction temperature. The effects of the package structure on the thermal performance are under more detailed simulation.

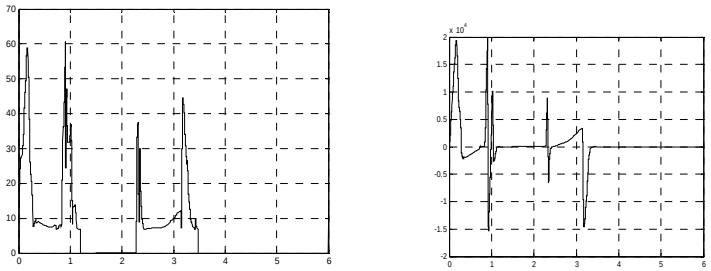

(a) Motor phase current (A) (b) Motor input power (W)

Figure 8. Absolute value of motor phase current ($|I|$) and motor input Power (W)

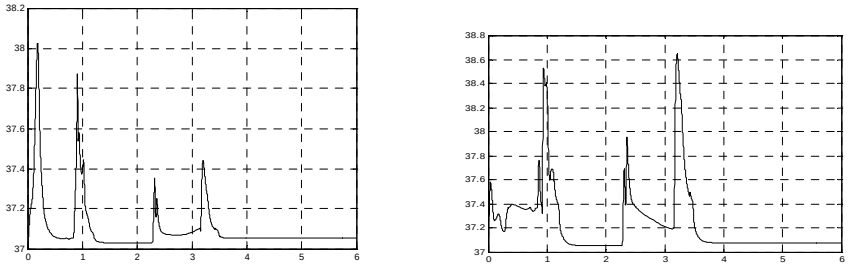

(a) JFETs (b) Schottky diodes

Figure 9. Junction temperature (°C) of SiC devices

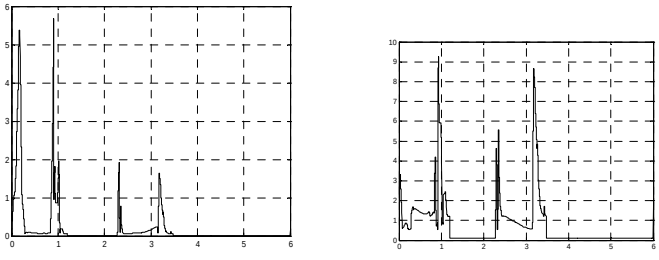

(a) SiC JFETs (b) SiC Schottky diodes

Figure 10. Power Loss (per component) in Watts

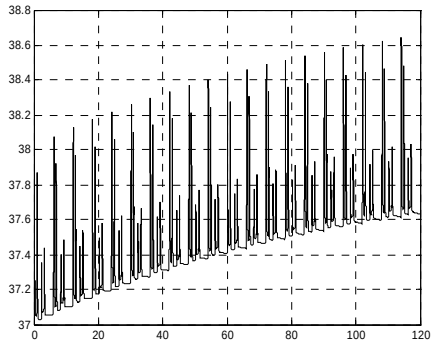

(a) SiC JFETs

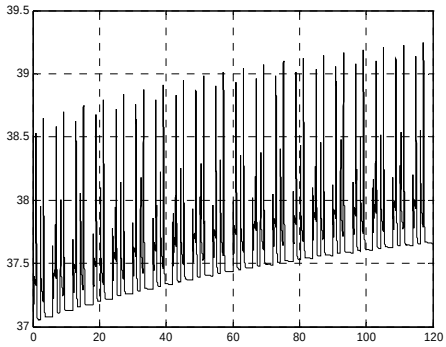

(b) SiC Schottky Diodes

Figure 11. Junction Temperature (20 cycles) (°C) by using a heatsink of R_{ca}= 0.1 K/W and τ_{ca} = 1000 s

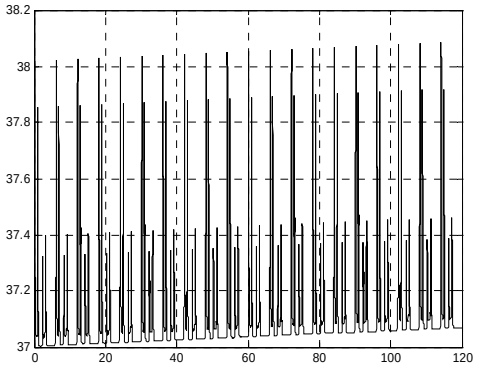

(a) SiC JFETs

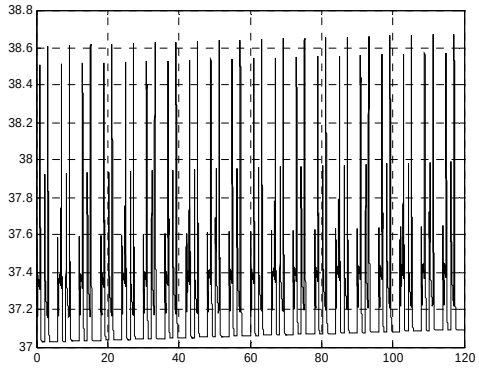

(b) SiC Schottky Diodes

Figure 12. Junction Temperature with a more efficient heatsink (20 cycles) (°C) by using a heatsink of R_{ca}= 0.156 K/W and τ_{ca} = 102 s

Table 3 Maximum/average temperatures and power loss of SiC and Si devices

Material		Maximum temperature for 1st cycle (°C)		Average temperature rise per cycle (°C)		Maximum power loss (W)	Average power loss (W)	Inverter efficiency
		JFETs/ MOSFET	Diodes	JFETs/ MOSFET	Diodes			
R_{ca}= 0.156 K/W	SiC	38.026	38.651	0.054	0.078	89.50	5.92	99.48%
	Si	71.887	111.97	0.715	2.827	1790.6	77.69	93.13%
R_{ca}= 0.1 K/W	SiC	38.020	38.610	0.005	0.030	89.50	5.92	99.48%
	Si	71.741	111.24	0.079	2.191	1790.6	77.69	93.13%

5. Summary

1. The power inverter based on emerging SiC devices are expected to provide higher efficiency and reduced size/weight. Feasibility of a SiC converter has been demonstrated through (1) Circuit design; (2) System modeling; (3) Packaging and thermal management. Two commercially available devices, SiC VJFETs and Schottky diodes are used for the inverter prototype. Integration of circuit design, thermal management and high-temperature gate drive that is under investigation will enable SiC converters and their applications.

2. The power loss modeling and simulation of SiC power devices and the SiC inverter has been conducted, in order to demonstrate both the device-level (e.g. junction temperature) and the system-level impacts (e.g. power loss) of a SiC-based inverter as compared with a Si-based inverter. The simulation results show that the SiC-based inverter has a much lower junction temperature, much less power loss, and much enhanced energy efficiency.

3. A novel thermal management approach for the SiC devices, which is based on the AlN package and carbon foam heatsink, has been designed and developed. The thermal management can work at higher temperatures and with more efficient heat dissipations the currently available products.

6. Reference

1. Cooper, J. A., Jr., et al., "Status and Prospects for SiC Power MOSFETs," *IEEE Transactions on Electron Devices*, 49(4): 658-663, April 2002.
2. Levinshtein, M. E., et al., "Fast Switch-Off of High Voltage 4H-SiC npn Bipolar Junction Transistor from Deep Saturation Regime," *Solid-State Electronics*, 48(3): 491-493, 2004.
3. Heinz L., "4,5kV 4H-SiC diodes with ideal forward characteristic," *ISPSD'01: Proceedings of the 13th International Symposium on Power Semiconductor Devices & ICs*, Osaka, Japan, June 4-7, 2001.
4. Ozpineci, B., et al., "Effects of Silicon Carbide (SiC) Power Devices on PWM Inverter Losses," *The 27th Annual Conference of the IEEE Industrial Electronics Society*, Denver, Colorado, USA, November 29–December 2, 2002.
5. Ozpineci, B., et al., "Testing, Characterization, and Modeling of SiC Diodes for Transportation Applications," *33rd Annual IEEE Power Electronics Specialists Conference (PESC'02)*, Cairns, Australia, July 23-27, 2002.
6. Ozpineci, B., et al., "System Impact of Silicon Carbide Power Devices," *International Journal of High Speed Electronics and Systems*, 12(2): 439-448, 2002.
7. Tolbert, Leon et al., "Impact of SiC Power Electronic Devices for Hybrid Electric Vehicles," *2002 Future Car Congress Proceedings*, June 3-5, 2002, Arlington, Virginia. (SAE Paper Number 2002-01-1904).
8. Alexandrov, P. et al., "Inductively-loaded half-bridge inverter characterization of 4H-SiC merged PiN/Schottky diodes up to 230A and 250C", *Electronics Letters*, 37: 1261-1262, 2001
9. Allebrand, B. et al., "On the possibility to use SiC JFETs in Power Electronic circuits", *9th European Conference on Power Electronics and Applications*, Brussels, Belgium: EPE Assoc, 2001. p. 9
10. Zhao, H.J. et al., "A novel high-voltage normally-off 4H-SiC vertical JFET," *Materials Science Forum*, 338-342(2): 1223-6, 2000.
11. Friedrichs, P. et al., "Static and dynamic characteristics of 4H-SiC JFETs designed for different blocking categories," *Materials Science Forum*, 338-342(2): 1243-6, 2000.
12. Ozpineci, B., et al., "Comparison of Wide Bandgap Semiconductors for Power Electronics Applications,"*10th European Conference on Power Electronics and Applications - EPE 2003*, Toulouse, France, September 2-4, 2003.
13. Ozpineci, B., et al., "Testing, Characterization, and modeling of SiC Diodes for Transportation Applications," *Power Electronics Specialists Conference*, Cairns, Australia, June 23–27, 2002.
14. Lin, Zhigang et al., "The Package and Heatsink Techniques for High Temperature, High Power Density Electronics", *23rd Army Science Conference*, Orlando, Florida, USA, December 2-5, 2002.
15. Lin, Zhigang et al., "Development of a High Temperature, High Power Density Packaging System: a Novel Microchannel Heat Sink", *HiTEC (High temperature Electronics Conference)*, Albuquerque, New Mexico, USA, June 2-6, 2002
16. Lin, Zhigang et al., "An AlN-based High Temperature Package for SiC Devices: Materials and Processing", *2005 IEEE/CPMT 10th International Symposium and Exhibition on Advanced Packaging Materials Symposium: Processing, Properties and Interfaces*, Irvine, California, USA, March 16-18, 2005.
17. Chinthavali, Madhu, et al., "Enhanced Power Electronic Devices with Wide Bandgap Semiconductors", *Workshop on Frontiers in Electronics*, Palm Beach, Aruba, December 21, 2004.
18. Lin, Zhigang, et al., "Strength-enhanced Carbon Foam Materials for Heat Exchanger Applications", *29th Annual Conference on Composite, Materials and Structures*, Cocoa Beach, Florida, USA, January 24-27, 2005.